International Journal of Engineering Research & Technology (IJERT)
ISSN: 2278-0181
Vol. 3 Issue 2, February - 2014

Geometry Optimization of Aerodynamic Add-on Devices Using the Globalized and Bounded Nelder-Mead Algorithm

A. Ait moussa, R.Yadav, J. Baker, J. Fischer
Department of Engineering and Physics
University of Central Oklahoma
Edmond, Oklahoma, USA

***Abstract*—The rising trend in fuel prices has led to growing concern about vehicle fuel economy, and viscous drag is one of the main factors. Improvement in fuel efficiency can be achieved at a relatively low cost by installing aerodynamics devices to streamline vehicles and reduce drag. We report here an efficient numerical technique to automatically optimizing the geometry of suchdevices. The technique combines shape optimization, geometric modeling, and Finite element analysis (FEA). To assess the validity of our optimization algorithm, we compare our optimization results against known test cases similar to the configurations in hand. We use this method to examine how effective add-on devices in reducing drag on a simple model of a commercial truck.**

Keywords—Aerodynamics, Fluid dynamics, Optimization, Golobalized and bounded Nelder-Meda, CFD based optimization

I. INTRODUCTION

In the history of aerodynamic research around bluff bodies[1, 2] such as trucks, trailers and sport utility vehicles (SUVs), it has always been observed that the shape of the body is one of the main obstacles to improving fuel economy[3]. The air flow produces pressure unbalance between the fore and aft facing surfaces of the vehicle. This pressure difference along with vortex shedding and skin friction cause drag [4–6], thereby increasing the fuel consumption. Improvement in fuel efficiency can however be achieved at a relatively low cost by installing aerodynamic add-on devices to streamline the body shape and reduce drag [19]. For maximum performance, the number and geometrical parameters of these devices must be optimized.

Conventional methods for finding optimal geometric configurations of aerodynamic devices for drag reduction rely on experimentation and/or computational simulation. The analysis is done iteratively by varying one of the device's geometrical parameters with the hope of maximizing drag reduction. Cooper [7] for example, investigated the effect of tail gate position of a commercial truck. He conducted full scale experimental tests and presented the results with computational fluid dynamics (CFD) analysis to visualize the flow structure of tailgate up and tailgate off at zero degree yaw angle. The results showed that the removal or lowering of the tailgate increases the aerodynamic drag. Ha, Jeong, and Obayashi [8] carried out an experimental and computational study of the changes in the flow characteristics with variations in thebed geometry of a pickup truck. They found that the attachment of the bed flow to the upper part of the tailgate increases the drag coefficient when the bed geometry is unable to cover the downwashof the bed flow entirely. The same authors [9] examined drag reduction of a pickup truck by a rear flap add-on through CFD simulations and wind tunnel experiments. They concluded that rear downward flap was effective in reducing the drag coefficient through an increase in the flap length and the downward angle. Yang and Khalighi[10] were more concerned with the ability of CFD simulations and the two-equation k-epsilon turbulence model to capture steady flow around pickup trucks. They compared the data from CFD simulations with excremental data collected form Al-Garni, Bernal and Khalighi's experiments [11] and concluded that the steady state formulation was good enough to study vehicle aerodynamics. These cases and others not listed for brevity, simultaneously demonstrate the ability of CFD simulation to predict fluid flow around vehicles such as trucks, and how the experimental investigationstill the preferred choice in aerodynamics quest.

Drag optimization problems in general are multi-variable multi-constraint problems, and small changes in any of the geometrical parameters of the vehicle may lead to larger changes in aerodynamic flow. Rather than manually iterating design changes whether experimentally or via CFD simulation until all design requirements are met, an engineer can work more effectively by automating the design and simulation processes and allow an optimization algorithm to create a final design that meets the particular requirements. The technique introduced in this paper is based on this perception and will be discussed in more details in the next few sections.

This paper is divided into three major parts. In the first, we introduce the technique of optimization and components used in the process of computing and minimizing drag. Next, we benchmark and apply this technique to a generic model of a commercial truck customized with a rear cabin flap. In the final section we conclude with a summary and a discussion of future work.

II. THE COMPUTATIONAL TECHNIQUE

In this section, we shall describe the general structure of the computational technique used in the optimization that we apply to a specific system in section III. We shall present this general

IJERT

case first and then indicate briefly how the results will simplify for our special case.

A. The Optimization Technique

Techniques of constrained and unconstrained optimization are well known and studied in the literature [12–14]. Numerical algorithms can be broadly categorized into gradient-based methods and direct search methods. Gradient-based methods use first or second derivatives, while direct search methods such as the Nelder-Mead [15], do not use derivative information. Direct search methods tend to converge more slowly, but can be more tolerant to the presence of noise in the function and constraints. In this paper, the Nelder-Mead (N-M) algorithm is used for the purpose of reducing viscous drag.

The N-M method compares values of the objective function at a set of n + 1 points called a simplex where n is the number of design variables. Simplex vertices are changed through reflection, expansion, contraction, or shrinkage. The process is continued until the simplex converges to a local optimum. Thus, the local optimum found is dependent on the initial simplex.

The original N-M algorithm was designed for unconstrained optimization, but the variables in an engineering problem such as the one we are currently facing are usually constrained by upper and lower bounds (i.e. box constraints). To constrain The N-M optimization algorithm, we use a projection procedure on the box constrained variables [16, 17]. Projection of variables is mathematically specified by

$$x_i = \begin{cases} x_i^{lower\ \ bound} & if\ \ x < x_i^{lower\ \ bound} \\ x_i^{upper\ \ bound} & if\ \ x > x_i^{upper\ \ bound} \end{cases} \quad (1)$$

where x_i is a point sampled during the optimization.

Strictly speaking, Nelder-Mead is not a true global optimization algorithm; and may only lead to one or morelocal minima depending on the starting simplex. A global search however, can be performed by repeatedly restarting the N-M algorithm. To avoid finding the same local optima, the new initial points should be different and preferably far from previous initial points and already known local solutions. To this end, we use a variable variance probability density (VVP) [17] to identify a point reasonably far from the known local minima and initial starting points then construct a simplex from it and restart the local optimizer for the next optimum. More detail about the VVP can be found in appendix A.

The diagram in Fig.1 represents the scheme used in the implementation of the Globalized and Bounded Nelder-Mead algorithm (GBNM) and the repetitive restarts needed to reach global minimum. This is the same restart scheme used by Luersenand Riche[16]. We start with a fixed number of random vertices; these are the initialpoints. We then identify the vertex with the largest probability density; this is the vertex with the largest distance to the closest neighbor. At this point we use a probabilistic restart by constructing an initial simplex from this point of size equal to 20% the domain size. We then proceed with the bounded Nelder-Mead optimizer and identify the first local optimum. We stop the N-M algorithm when the simplex is small, or flat. A simplex is small when.

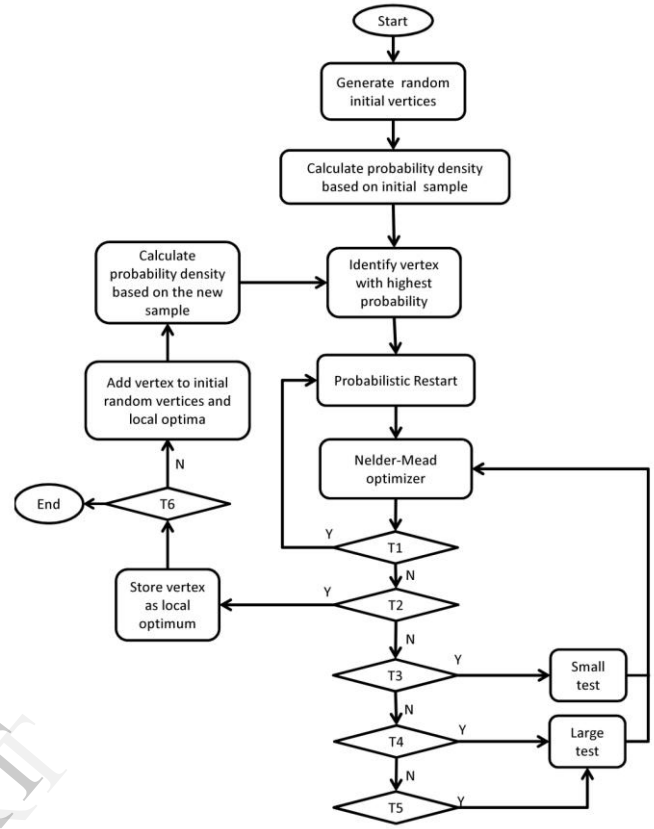

Figure 1: GBNM restarts schematics.T1: (this point is already known as a local optimum). T2: (vertex ix a local optimum). T3: (large test or probabilistic and not return to the same point and point on the bound). T4: (small test and not return to the same point and not on the bunds). T5: (N-M stopped by maximum number of iterations). T6: (maximum number of analyses is reached.

$$max\left(\left|\frac{x_i^{k+1} - x_i^k}{x_i^u - x_i^l}\right|\right) < \epsilon_1 \quad (2)$$

where k is the number of iterations, subscripts u and l represent the upper and lower bound on variable x_i, andϵ_1 is a predetermined small number.

Similarly, a simplex is flat when

$$|f_H - f_L| < \epsilon_2 \quad (3)$$

wheref_H and f_L are the highest and lowest function values at the current simplex, and ϵ_2 is a given small number.

The local optimum is then stored and used with the initial random points and any prior stored optima to update the probability density from which we identify the next best vertex and use the same probabilistic restart with a polyhedron of size equal to 20% the domain size. There may be cases however, when the new optimum is identical to one of the stored optima;that the maximum number of iterations in the N-M is reached; or that one or more of the simplex parameters are on the edge of the box constraint. In cases like these we proceed

IJERT

as indicated in the diagram. Small and large tests are used to restart the Nelder-Mead from the best pointof the current simplex with a polyhedron of size 2% and10% the domain size respectively

B. Program Structure

To achieve optimal values of drag coefficient (C_D) [1], we will be facing three parts of work; geometric modelling, finiteelement analysis (FEA) and mathematical programming. Different program files were developed for each part, and communication between these parts is manipulated by an interface. One of the most interesting features of the ANSYS Workbench software is the possibility to use it as a mere subroutine of any other external program. Parameters can be either directly passed or exchanged through external files. This flexibility allows us to build an interface between ANSYS and our external optimization algorithm, written in Visual Basics for application (VBA), where ANSYS is a finite element package used to calculate the objective function and constraints. For geometrical updates, we automate the SolidWorks Application Programming Interface (API) calls directly from our external optimization algorithm. The methodology schematics are shown in Fig.2. In the following the main parts are outlined.

Commands for adding the aerodynamics devices, for generating and storing the parasolid model are incorporated in a SolidWorks macro. This list of API calls is directly implemented into the optimization algorithm written in VBA.

Commands for uploading the parasolid model, for adding an enclosure to simulate fluid flow and for applying a Boolean operation to subtract the geometry of the truck from the enclosure are incorporated in a command file using the Java Python language for the ANSYS Design Modeler.

Commands for meshing, for adding inflation on the road and truck surfaces and for applying body sizing are incorporated in a command file using the Java Python language for the ANSYS Mesher.

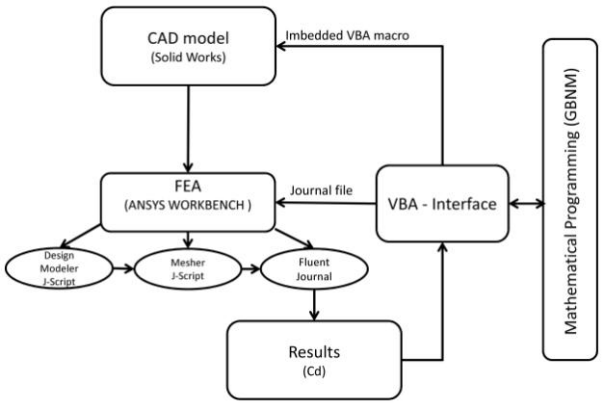

Figure 2: Methodology of geometry optimization

Commands for initializing the Fluent computation and applying boundary conditions are incorporated in a Fluent journal file. Upon completion of the pre and post- processing stages, ANSYS provides results file which records the drag coefficient over the steps of the simulation, this information is stored in a files.out and returned to the interface. Communication with the ANSYS Workbench is made possible via a journal file.

For geometry optimization, we used the Globalized and Bounded Nelder-Mead optimization algorithm. The in- put parameters are read from an excel sheet. Results and geometrical updates are printed out on the same sheet to show optimization progress.

C. Finite Element Analysis Setup and Procedure

We used the Fluent analysis system in ANSYS Workbench. The model including aerodynamic devices were imported to the Design modeler, and aligned with a control volume. A half model was used to allow quicker solution of the model with a more refined mesh. The control volume size was set according to Fluent's best practice guide for vehicle analysis [18]. The computational domain in Fig.3 extended around three times the vehicle length to the front and five times to the rear. The width and height of the control volume were set so that the cross section of the vehicle did not exceed 1.5% of the domain area. A box was created around the vehicle and in the wake region to control the mesh size during the meshing process. The box extended about half a vehicle length in front, to the sides and to the top, and about a vehicle length in the wake. The model was then subtracted from the computational domain to limit the computational analysis to the rest of the control volume and vehicle boundaries.

ANSYS Workbench offers a robust and easy to use set of meshing tools. These tools have the benefit of being highly automated along with having a moderate to high degree of user control. Based on the analysis system utilized, the Mesher in ANSYS Workbench uploads a set of default parameters that will result in a mesh that is more favorable to the solver used. By means of global and local mesh controls, the user can easily modify the mesh parameters. In this paper we adopted a physicsbased meshing, the physics preference was set to CFD and solver to Fluent. An inflation layer was added over the surfaces of the vehicle and the road as shown in Fig.4; the prisms were grown with a first aspect ratio of 10 and a growth factor of 1.2 extruding 5 layers. Body sizing was used for mesh refinement around the vehicle and wake region. Triangular mesh elements were used on the surface to reduce the numerical diffusion and to align with the real flow near the model. The remainder of the computational domain was filledwith tetrahedral volume cells that were adjacent to the prism layers.

A velocity-inlet boundary condition was used to model the incoming flow. Fluent's best practice guide for vehicle analysis [18] recommends using a Realizable k-epsilon Model, and non-equilibriumwall-functions(NWFs).Fluent convergence criterion of 10^{-4} for the continuity equation was used.

IJERT

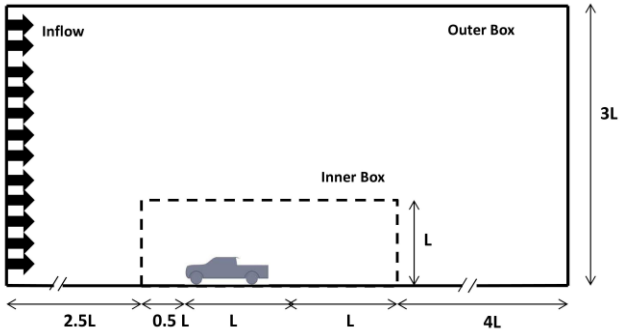

Figure 3: Simulation Box

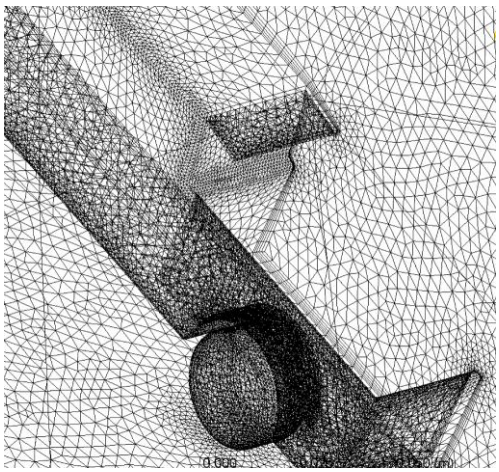

Figure 4: Boundary layer at a growth factor of 1.2, triangular mesh elements on the surface and tetrahedral volume cells in the reminder of the computational domain

III. APPLICATION

In this section we shall present the application of the technique introduced in section II to the case of a simple model of a commercial truck customized with a rear cabin flap.

The pickup truck model used was a 1/10th scale generic pickup truck without side mirrors, as shown in Fig.5. The bed length and bed height were 157.8 mm and H = 106.9 mm, respectively. The cabin flap was added and merged at the rear edge of the roof. The flap length (l) normalized by the cabin back height (H) and the downward angle (θ) measured from the horizontal were considered as the design variables. The tailgate height was h = 72.6 mm. The free stream velocity was set to 30 m/s, and the Reynolds number was calculated based on the overall model length to be Re = 7.95×10^5. The stopping criteria for the Nelder-Mead were $\epsilon_1 = \epsilon_2 = 10^{-3}$ for the small and flat simplex respectively. The maximum number of iterations in the Nelder-Mead was set to 50. The box constraints for the length and flap orientation were set to $0.1H < l < 0.3H$ and $0 < \theta < \pi/4$. We started with 10 random initial vertices over the domain of the analysis, and the optimization was performed up to 30 analyses. The optimum points were rounded off to10^{-2}.

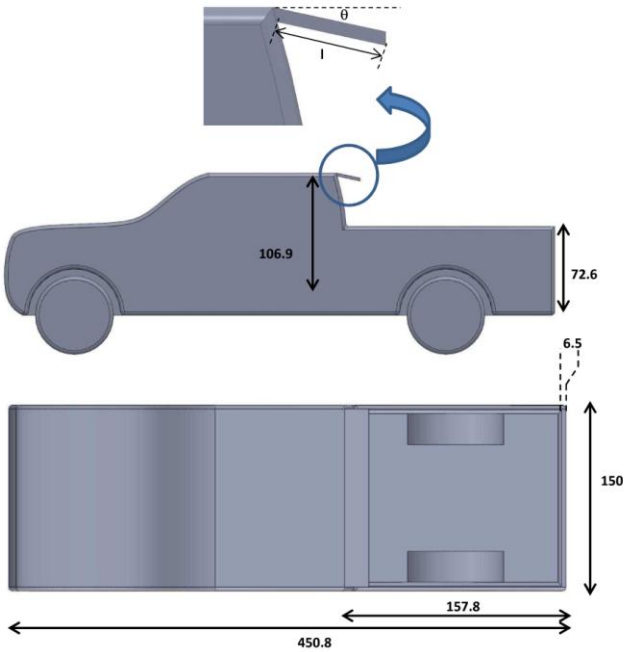

Figure 5: Truck model. Top view (bottom), side view (middle). Flap (top).

A. *Discussion of Results*

Table.I, shows five local minima, although there are around twenty other local solutions found during the optimization process that a designer can select from. In this respect, the optimization is comparable to an evolutionary procedure that provides a family of optimal solutions instead of just one specific solution. This feature is important especially for multi-objective optimization.

The results of table.I,prove that drag reduction is achievable at different lengths with slightly better results at larger flap lengths. The flap orientation however, seems to converge in all cases to values around 12 degree as measured from the horizontal and down. This is similar to the results of Ha, Jeong, and Obayashi[9]. There, they used a similar truck model, although with a wider tailgate. They then fixed the flap length in each analysis, and vary the angle to find that a maximum reduction can reached at an angle around 12 degrees.

To understand the underlying causes of these results, we plotted the pressure coefficients on the symmetry plane of the back surface of the cabin in Fig.6, as well as the front and back surfaces of the tailgate in Figs.7&8. The flap increased the cabin surface area and moved the reattachment point over the tailgate away from the bed as can be depicted in the inserts of Figs.9&10. As a result, the recirculating flow behind the cabin was reduced and its core shifted slightly toward the tailgate. The lesser the recirculation over the bed, the better the pressure on the cabin back and inside surface of the tailgate which explains the results of Figs.6&8. With the cabin flap, the flow separates at the outer edge of the tailgate and two noticeably counter rotating vortices are formed. The core of these vortices are farther from the tailgate compared to the case without cabin flap, which explains the slight improvement in the pressure over the tailgate back as depicted in Fig.7. Overall, the cabin flap reduced the pressure difference between the fore and after facing surfaces of the vehicle which thereby reduced drag.

IJERT

TABLEI:Optimum designobtainedbyGBNM

l(*H*)	$\theta(^o)$	%reduction
0.15	12.0	5.10
0.19	12.5	5.39
0.22	12.4	5.82
0.24	12.2	6.03
0.26	12.2	6.03

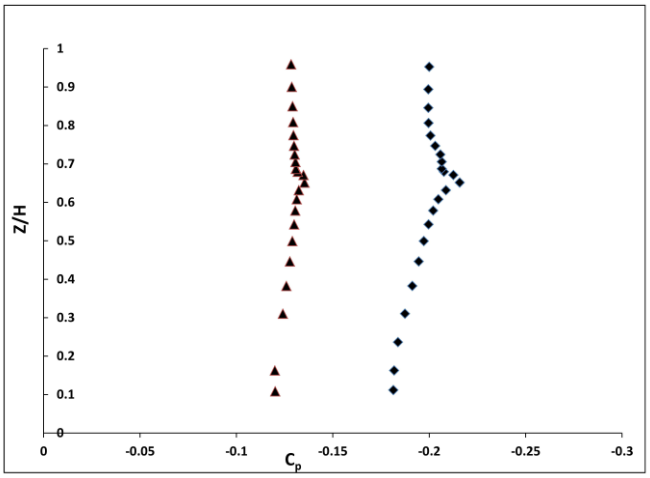

Figure 6: Pressure coefficient distribution (Cp) on the symmetry plane of the back surface of the cabin, the height (Z) is measured from the truck bed. (triangle: cabin with flap, l = 0.24 H and θ = 12.2°), and (rectangles: cabin without flap).

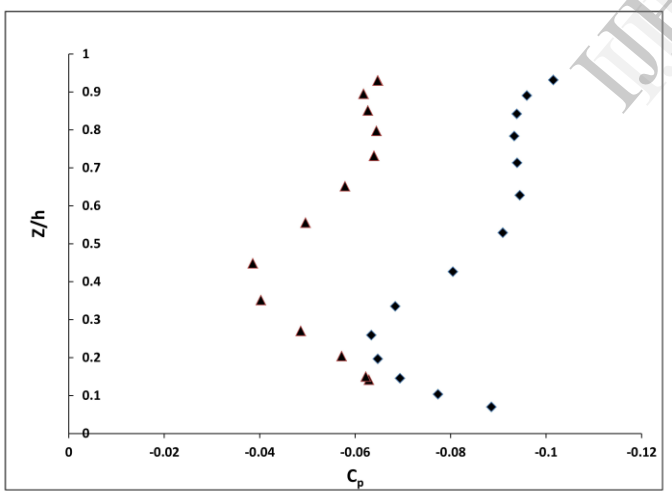

Figure 7: Pressure coefficient distribution (Cp) on the symmetry plane of the back surface of the tailgate, the height (Z) is measured from the truck bed. (triangle: cabin with flap, l = 0.24 H and θ = 12.2°), and (rectangles: cabin without flap).

IJERT

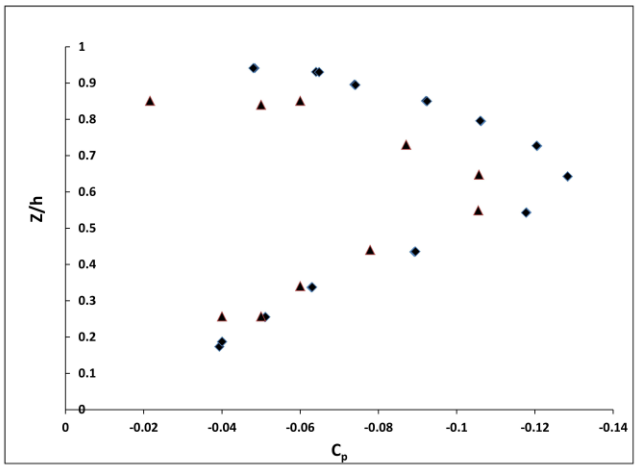

Figure 8: Pressure coefficient distribution (Cp) on the symmetry plane of the inside surface of the tailgate, the height (Z) is measured from the truck bed. (triangle: cabin with flap, l = 0.24 H and θ = 12.2°), and (rectangles: cabin without flap).

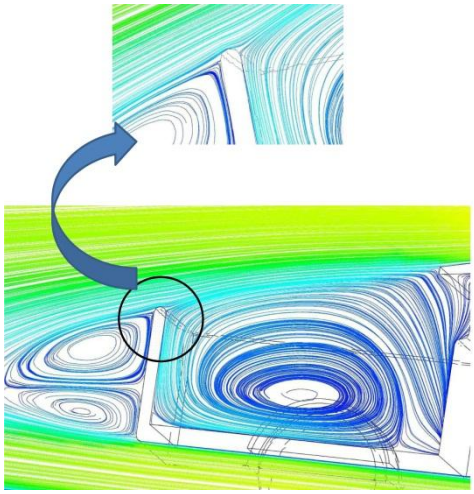

Figure 9: Streamlines colored by the pressure coefficient around the bed in the symmetry plane for the model truck with flap, l = 0.24 H and θ = 12.2°. The insert visualizes the flow attachment over the tailgate. (CFD data)

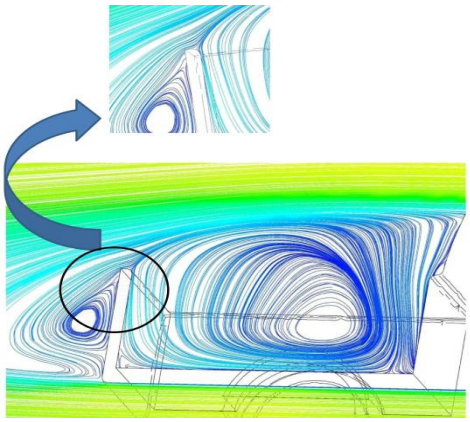

Figure 10: Streamlines colored by the pressure coefficient around the bed in the symmetry plane for the model truck without flap l = 0.24 H and θ = 12.2°. The insert visualizes the flow attachment over the tailgate. (CFD data)

IV. CONCLUSION AND FUTURE WORK

In this paper, we introduced a robust technique that combines mathematical programming; geometrical modeling and finite element analysis to optimize the geometry of aerodynamic add-on devices as they apply to road vehicles. To benchmark and test the robustness of the technique, we considered optimizing the length and orientation of a flap of fixed thickness merged to the back of the cabin of a simple model of a commercial truck. The evolutionary and constrained aspect of the technique produced a family of optimal solutions that a designer can choose from. The results were compared to other experimental and computational results and were proven to be consistent. The technique can further be used to optimize the geometry of other additional devices such as a tailgate flap since this may improve the pressure behind the tailgate as well as a combination of a cabin and tailgate flaps.

The methodology introduced in this paper can be broadened to several other engineering problems where fluid flow and geometrical or other physical constraints are to be met. The sequential use of mathematical programming, computational fluid dynamics and computer- aided design tools can for example, be utilized to improving the design of ventricular assist devices (VADs), where a compromise between the hydraulic performance and health related complications due to high stress rates is a major issue.

ACKNOWLEDGMENTS

The first author would like to express his gratitude to the office of research and grants at the University of Central Oklahoma (UCO) for the financial support during this research.

APPENDIXA:VARIABLEVARIANCE PROBABILITYDENSITY(VVP)

The variable variance probability (VVP) density is based on the minimum distance to the points already sampled and is represented as

$$\Phi(x) = \frac{1}{\sqrt{2\pi}\sigma}\left(1 - e^{d_{min}^2/2\sigma^2}\right) \qquad \text{(A1)}$$

$$d_{min} = \underbrace{min}_{i=1,\ldots,m}\left\{d_i = \sqrt{\sum_{k=1}^{n}\left(\frac{x_{k,i} - x_k}{x_{k,u} - x_{k,l}}\right)^2}\right\}$$

Where Φ(x) is the sampling probability of a point x, n is the number of design variables, xi is a point previously sampled, and m is the number of points already sampled. Length di is the non-dimensional distance between point x and point xi.

The variance of the normal probability density, which is updated in each restart, is given by:

$$\sigma = \frac{1}{3\sqrt[n]{m}} \qquad \text{(A2)}$$

The variance is gradually decreasing when the number of sampled points is increased.

REFERENCES

[1] W.H. Hucho, Aerodynamics of Road Vehicles, 4th Edition, SAE International, 1998

[2] Sovran, G., et al. (ed), Aerodynamic drag mechanisms of Bluff Bodies and Road Vehicles, Plenum Press, New York, 1978

[3] Hucho, W.-H., Sovran, G., Aerodynamics of Road Vehicles, Vol. 25: 485-537, 1993

[4] Achenbach, E., Distribution of Local Pressure and SkinFriction around a Circular Cylinder in Cross-Flow up to5×10^6, Journal of Fluid Mechanics, Vol. 34, Pt.4, 1968

[5] Von Karman, Theodore, "Turbulence and Skin Friction", J. of the Aeronautical Sciences, Vol. 1, No 1, 1934, pp.1-20.

[6] Anderson, John D (2001) Fundamentals of Aerodynamic3rd Edition, McGraw-Hill. ISBN 0-07-237335-0

[7] Cooper, K., Pickup trucks Aerodynamics - Keep your tailgate Up, SAE Paper No. 2004-01-1146, 2004.

[8] Ha,J., Jeong, S. and Obayashi, S. (2010). Flow characteristics of a pickup truck with regard to the bed geometry variation. P roc. Inst. Mech. Eng. D, J. Automobile Engineering, 224, 881891.

[9] J.Ha, S.Jeong and S.Obayashi, Drag reduction of a pickup truck by a rear downward flap, International Journal of Automotive Technology, Vol. 12, No. 3, pp. 369374 (2011)

[10] Yang, Z., and Khalighi, B., CFD Simulation for FlowOver Pickup Trucks, SAE Paper No. 2005-01-0547, 2005

[11] Al-Garni, A., Bernal, L., and Khalighi, B., Experimental investigation of the Near Wake of a Pick-up Truck, SAEPaper No. 2003-01-0651, 2003.

[12] E.K.P. Chong and S.H. Zak. An Introduction to Optimization. John Wiley & Sons, Inc. New York: 1996.

[13] L.R. Foulds. Optimization Techniques. Springer-VerlagNew York Inc. New York: 1981.

[14] J.C. Lagarias, J. A. Reeds, M. H. Wright, and P.E.Wright, "Convergence Properties of the Nelder-Mead Simplex Method in Low Dimensions," SIAM Journal of Optimization, Vol. 9, Number 1, pp.112-147, 1998.

[15] Nelder, J.A. and R. Mead. A Simplex Method for Function Minimization. The Computer Journal 7 (1965):308313.

[16] Luersen, M.A. and Riche, R.L. (2004). Globalized Nelder-Mead Method for Engineering Optimization, Computers and Structures, 82: 22512260.

[17] Ghiasi H, Pasini D, Lessard L (2008) Constrained globalized Nelder-Mead method for simultaneous structural and manufacturing optimization of a composite bracket. J.Compos Mater 42(7):717736

[18] M. Lanfrit, Best Practice Guidelines for Handling Auto-motive External aerodynamicswithFluent,Version1.2, http://www.fluentusers.com,2005

[19] Jeff, H. (2002). Aerodynamic drag of a compact SUV as measured on-road and in the wind tunnel. SAE Paper No. 2002-01-0529.

IJERT